ANTIMICROBIAL AGENTS AND CHEMOTHERAPY, Jan. 2010, p. 280–287 Vol. 54, No. 1
0066-4804/10/$12.00 doi:10.1128/AAC.00914-09

Mitochondrial DNA Depletion and Respiratory Chain Activity in Primary Human Subcutaneous Adipocytes Treated with Nucleoside Analogue Reverse Transcriptase Inhibitors▽

Metodi V. Stankov,[1] Thomas Lücke,[2] Anibh M. Das,[2] Reinhold E. Schmidt,[1] and Georg M. N. Behrens[1]*

Clinic for Immunology and Rheumatology[1] and Clinic for Paediatric Nephrology, Hepatology and Metabolic Disorders,[2] Hannover Medical School, Carl-Neuberg-Str. 1, 30625 Hannover, Germany

Received 2 July 2009/Returned for modification 28 August 2009/Accepted 30 September 2009

Mitochondrial dysfunction as a consequence of mitochondrial DNA (mtDNA) depletion due to therapy with nucleoside analogue reverse transcriptase inhibitors (NRTI) has been proposed as a pathogenic mechanism leading to lipoatrophy in HIV-infected patients. The aim of our study was to investigate the impact of NRTI treatment on mtDNA abundance and the activities of respiratory chain complexes in primary human subcutaneous preadipocytes (phsPA). We studied adipocyte phenotypes, viability, and differentiation (CCAAT/enhancer-binding protein α [C/EBPα] and peroxisome proliferator-activated receptor γ [PPARγ] expression) and adiponectin production, mtDNA content, mitochondrial membrane potential, mitochondrial mass, and respiratory chain enzyme and citrate synthase activities in both proliferating and differentiating phsPA. Cells were exposed to zidovudine (6 μM), stavudine (d4T; 3 μM), and zalcitabine (ddC; 0.1 μM) for 8 weeks. NRTI-induced mtDNA depletion occurred in proliferating and differentiating phsPA after exposure to therapeutic drug concentrations of d4T and ddC. At these concentrations, ddC and d4T led to an almost 50% decrease in the number of mtDNA copies per cell without major impact on adipocyte differentiation. Despite mtDNA depletion by NRTI, the activities of the respiratory chain complexes, the mitochondrial membrane potential, and the mitochondrial mass were found to be unaffected. Severe NRTI-mediated mtDNA depletion in phsPA is not inevitably associated with impaired respiratory chain activity or altered mitochondrial membrane potential.

Nucleoside reverse transcriptase inhibitors (NRTI) have been proposed to affect mitochondrial DNA (mtDNA) replication and to cause mitochondrial toxicity both in vitro and in vivo (19, 27). Therefore, mitochondrial toxicity has been hypothesized as a mechanism contributing to the development of fat loss and insulin resistance, both elements of the lipodystrophy syndrome seen in HIV-infected patients undergoing antiretroviral combination therapy (4). A number of studies have identified stavudine (d4T) as a particular risk factor (7, 13, 14, 23). Interestingly, preserved cytochrome *c* oxidase (complex IV) activity in adipose tissues of HIV-infected patients with lipoatrophy, despite mtDNA depletion, has been documented previously (15). In addition, endocrinological studies demonstrated decreased serum adiponectin levels in HIV-infected subjects with fat redistribution caused by highly active antiretroviral therapy (1) and in a murine model of lipoatrophy and suggested the involvement of this adipokine in lipodystrophy syndrome (36). However, despite the numerous studies demonstrating an effect of NRTI therapy on mtDNA contents in various tissues, there are fewer data demonstrating mtDNA depletion as a relevant cause for mitochondrial and adipocyte dysfunction. The proof of this association in relation to human adipocytes will be relevant for the understanding of the pathogenesis of lipoatrophy (4).

The majority of the in vitro studies so far have been performed using murine adipocyte cell lines (3T3-L1 and 3T3-F442A) or human nonadipocyte models such as fibroblasts (6) and hepatic tumor cell lines (e.g., HepG2) (35). These approaches harbor limitations, as murine cell lines do not account for possible interspecies differences in NRTI uptake efficiency and metabolism and tumor cell lines may have intrinsically disturbed mitochondrial function and dependency on mtDNA content. Using the 3T3-L1 murine cell line, we previously found the coexistence of severe mtDNA depletion (up to 80%) with unimpaired respiratory chain activity (28). However, in that model, we did not study mitochondrial enzyme activities in differentiating and fully differentiated adipocytes, which represent a substantial portion of adipocyte depots. In this study, we aimed to investigate NRTI-induced mtDNA depletion as a relevant cause for mitochondrial and adipocyte dysfunction in a system corresponding as closely as possible to the in vivo situation. We therefore designed experiments using primary human subcutaneous preadipocytes (phsPA).

MATERIALS AND METHODS

Cells and cell lines. Human subcutaneous fat tissue samples from the abdominal region of HIV-seronegative donors were kindly provided by Kerstin Reimers, Clinic for Plastic, Chiroplastic and Restorative Surgery, Hannover Medical School. The experiments were performed with pooled preadipocytes from different donors in order to decrease issues with person-to-person variability, as is routinely done for commercially available phsPA (37) used by others in similar

* Corresponding author. Mailing address: Clinic for Immunology and Rheumatology, Hannover Medical School, Carl-Neuberg-Strasse 1, 30625 Hannover, Germany. Phone: 49 (0) 511 532 5713. Fax: 49 (0) 511 532 5324. E-mail: behrens.georg@mh-hannover.de.

▽ Published ahead of print on 5 October 2009.

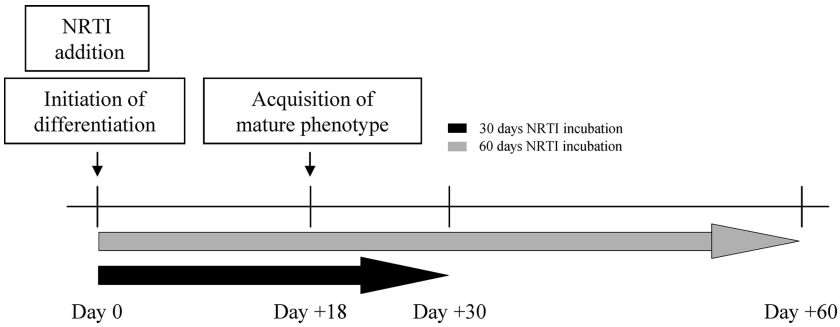

FIG. 1. Experimental schedule. phsPA were either kept proliferating or induced to differentiate in the presence of 6 μM AZT, 3 μM d4T, and 0.1 μM ddC or vehicle on the day designated day 0 and cultured for up to 30 or 60 days. On day 18, the phsPA reach a plateau in the acquisition of a mature phenotype.

experiments (18). phsPA used in differentiation experiments were at passage numbers up to 4, according to commercially available protocols (37).

Isolation and maintenance of phsPA were carried out essentially as described previously (29). phsPA were maintained in low-glucose Dulbecco's modified Eagle medium (DMEM; 1 g/liter glucose)–Ham F-12 medium (1:1) containing 10% fetal bovine serum and 172 μM L-ascorbic acid 2-phosphate sesquimagnesium salt hydrate (A-2-P). For differentiation, preadipocyte medium was supplemented with a mixture of hormones containing 520 μM 3-isobutyl-1-methylxanthine (for the first 7 days only), 1 μM dexamethasone, 167 nM insulin, and 100 μM indomethacin (indometacin). During the first 18 days of differentiation, low-glucose DMEM was replaced with high-glucose DMEM containing 4.5 g/liter glucose. Under these conditions, at least 70% of the cells differentiated, as estimated by the acquisition of a mature phenotype and cytoplasm filled with multiple lipid droplets (visualized by oil red O staining). Primary human subcutaneous fibroblasts isolated and maintained as explained earlier (20) were cultured in a similar manner and served as a negative control for differentiation. Preadipocytes were kept proliferating by being split before they reached confluence. All drugs were dissolved in dimethyl sulfoxide, and concentrations were around the maximum concentrations of the drugs in serum (C_{max}) achieved under therapeutic conditions (for zidovudine [AZT], 6 μM; for d4T, 3 μM; and for zalcitabine [ddC], 0.1 μM), as discussed in reference 29. The highest concentration of the solvent used in the incubation experiments (0.1% DMSO) did not affect cellular viability. Cell numbers and viability were determined microscopically by trypan blue staining after the cells were trypsinized.

NRTI treatment. phsPA were induced to differentiate in the presence or absence of levels equivalent to therapeutic C_{max} of AZT (6 μM), d4T (3 μM), and ddC (0.1 μM), which were added together with the differentiation stimulus at baseline, designated day 0 (Fig. 1). A plateau in the acquisition of a mature phenotype was observed at day 18. Drug treatment was extended to either day 30 or day 60 (Fig. 1).

Cell viability. The numbers of dead and viable cells were determined microscopically using trypan blue exclusion. Every fifth day, when the culture medium was changed, the percentage of dead cells was calculated, and the final calculation of viable cells was made by excluding the cumulative percentage of dead cells for the entire period of incubation with NRTI.

Adipocyte staining with oil red O. Adherent cells were fixed in 10% formalin, washed, and stained with a solution (60% isopropanol and 40% water) of 0.21% (wt/vol) oil red O (Sigma-Aldrich, Munich, Germany). Oil red O staining was studied by conventional fluorescence microscopy. For objective quantification of triacylglyceride contents, cells were dried and oil red O was extracted with 100% isopropanol and photometrically measured at 495 nm.

RNA preparation and real-time quantitative PCR. Total RNA extraction was done using an RNeasy lipid tissue minikit (Qiagen, Hilden, Germany). cDNA was synthesized from total RNA in a 20-μl volume by using random nonamers, oligo(dT) primers, and an Omniscript reverse transcriptase kit (Qiagen, Hilden, Germany). The primers were designed using Primer3 software (25). Real-time quantitative PCR analyses for the genes encoding peroxisome proliferator-activated receptor γ (PPARγ), CCAAT/enhancer-binding protein α (C/EBPα), and adiponectin were performed with a final volume of 25 μl by using a QuantiTect SYBR green PCR kit (Qiagen, Hilden, Germany) in an iCycler system. The following human-specific primers were used: C/EBPα forward primer, 5′-GACCTAGAGATCTGGCTGTG-3′, and reverse primer, 5′-GAGCAAAACCAAAACAAAAC-3′; PPARγ forward primer, 5′-AAGC GATTCCTTCACTGATA-3′, and reverse primer, 5′-GTGGAGTAGAAAT GCTGGAG-3′; and adiponectin forward primer, 5′-TTCTGATTCCATACC AGAGG-3′, and reverse primer, 5′-GATCTCCTTTCTCACCCTTC-3′. Amplifications were performed in optical 96-well plates by using a spectrofluorometric thermal cycler (iCycler; Bio-Rad, Munich, Germany). Genes of interest and reference gene products were amplified separately, using identical cycling conditions. Initial incubation at 95°C for 15 min was carried out for the activation of HotStar *Taq* DNA polymerase, and then 42 cycles of 94°C (15 s) for denaturation, 55°C (30 s) for annealing, and 72°C (30 s) for extension were performed. To ensure that a single amplicon of the expected size was obtained as a result of the PCR, the products were evaluated by melting-curve analysis and examined on ethidium bromide-stained agarose gels. The absence of residual DNA from our RNA preparations was ensured by using PCRs without reverse transcription. To determine PCR efficiency, reverse-transcribed RNA in serial dilutions (1, 1/5, and 1/25) was amplified, a standard curve was created by plotting cycle threshold values as a function of the starting amount of reverse-transcribed RNA, and the slope of the graph was used for efficiency calculation using the iCycler software. The relative quantification for any given gene was performed after dividing the standard curve value for the given gene *A* by that for the calibrator (transferrin receptor or beta-actin) gene *B* in treated and control cells. The effect of the particular NRTI was calculated by comparing mean values obtained from three independent experiments. In each of three experiments, RNAs from three independent culture plates were isolated and pooled. The pooled RNA was reverse transcribed, and cDNA was obtained by three separate reactions. These cDNAs were again pooled and measured in triplicate by real-time PCR. The triplicate real-time PCR results from three independent experiments were used for statistical evaluation. These results were compared to the mean value for the control cells subjected to the same procedure.

mtDNA studies. Real-time quantitative PCR analysis of mtDNA content was performed essentially as described previously for 3T3-L1 cells (28) by using human-specific primers. In order to calculate the absolute mtDNA copy numbers, serial dilutions of plasmids with known copy numbers were used.

Respiratory chain complexes. Activities of respiratory chain complexes were measured essentially as described previously for cultured fibroblasts (10) and murine 3T3-L1 cells (28). phsPA or adipocytes and their mitochondria were first broken by two 10-s periods of sonication using a Sonopuls probe sonicator (Bandelin Electronic, Berlin, Germany) with single pulses of 0.3 s and 20 W of power. Activities of oxidative phosphorylation chain complexes I and III, II and III, IV (cytochrome *c* oxidase), and V (ATP synthase) were measured at 37°C as described comprehensively for cultured fibroblasts (20). The activity of citrate synthase as a mitochondrial marker enzyme was analyzed as described elsewhere (11). Cellular protein was measured according to the method of Bensadoun and Weinstein (3). Positive controls of affected respiratory chain function were run as explained earlier (20).

Flow cytometric analyses of mitochondrial function and mitochondrial mass. To evaluate the integrity of mitochondrial functions, we used the cationic dye JC-1 assay kit according to the instructions of the manufacturer (Molecular Probes, Eugene, OR). Mitochondrial mass was measured using MitoTracker Green FM stain according to the instructions of the manufacturer (Molecular Probes, Eugene, OR). JC-1 and MitoTracker staining has been used previously for in vitro measurement of adipocyte mitochondrial membrane potential and

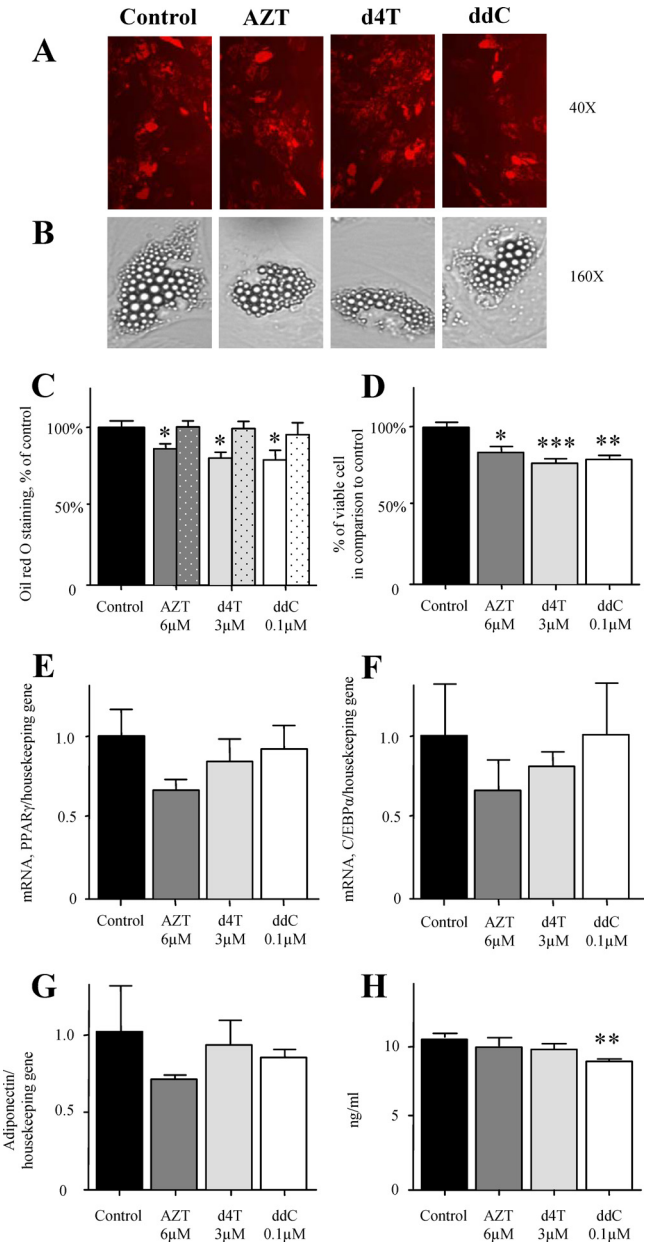

FIG. 2. Effects of NRTI on adipogenic conversion of phsPA. (A) The phenotypes of phsPA (oil red O-stained cells) were examined by conventional fluorescence microscopy on day 30 after the initiation of differentiation in the absence or presence of 6 μM AZT, 3 μM d4T, or 0.1 μM ddC. (B) The NRTI-treated cultures displayed phenotypes and numbers of triacylglyceride droplets similar to those in the control. Numbers to the right are original magnification values. (C) phsPA were stained with oil red O, and staining was quantified at 495 nm on day 30 after the initiation of differentiation in the presence or absence of AZT (6 μM), d4T (3 μM), or ddC (0.1 μM). Dotted bars represent results adjusted for the number of viable cells. (D) Cumulative cell death over the whole period was used in order to calculate cell viability at the end of incubation with the drugs. (E and F) Effects of AZT (6 μM), d4T (3 μM), and ddC (0.1 μM) on the expression of the differentiation factors PPARγ (E) and C/EBPα (F) in differentiating phsPA. Preadipocytes were cultured in the presence of vehicle or NRTI from day 0, when they were induced to differentiate, until day 30. Total RNA was isolated on day 18 and reverse transcribed, and real-time PCR analysis was performed to assess expression levels of two transcription factors involved in a cascade during preadipocyte differentiation. (G and H) Analyses of the expression levels of adiponectin on day 30 (G) and the levels of adiponectin secretion into the medium during the last 5 days (days 25 to 30) of incubation with NRTI (H). Panels A and B show images representative of cell cultures from three independent experiments. Graphs C and D depict data from five independent experiments. Graphs E to G depict data from three independent experiments with triplicate samples per experiment. Graph H depicts data from three independent experiments. Values are means ± SEM. ANOVA with Bonferroni's post hoc analysis was performed for comparison. *, $P < 0.05$; **, $P < 0.01$; and ***, $P < 0.001$ for comparison to control data.

mass correspondingly (5). Flow cytometric analyses were performed using a FACSCalibur instrument (Becton Dickinson, Heidelberg, Germany).

Enzyme-linked immunosorbent assay. The Quantikine human adiponectin enzyme-linked immunosorbent assay, designed to measure human adiponectin levels in cell culture supernatants, was used according to the instructions of the manufacturer (R&D Systems, Wiesbaden-Nordenstadt, Germany). The measurement of adiponectin represented the result of five days of secretion from phsPA differentiated in the presence of different NRTI or a vehicle.

Statistics. The statistical analyses were done by using unpaired Student's *t* test. Comparisons of more than two groups were performed by analysis of variance (ANOVA) with Bonferroni's post hoc analysis. The level of significance was set at a P value of <0.05. All data are expressed as means ± standard errors of the means (SEM). All calculations were performed using SPPS 15.0 for Windows.

RESULTS

NRTI effects on differentiation-dependent triacylglyceride accumulation. To extend previous in vitro observations (26), phsPA were induced to differentiate in the presence or absence of levels equivalent to therapeutic C_{max} of AZT (6 μM), d4T (3 μM), and ddC (0.1 μM) added from day 0 until day 30 (Fig. 1). Examination of the oil red O fluorescence by conventional fluorescence microscopy revealed comparable results for NRTI- and vehicle-treated cells (Fig. 2A). Light microscopy confirmed unaffected acquisition of a characteristic mature adipocyte shape and the accumulation of lipid droplets (of similar sizes and numbers) in NRTI- and vehicle-treated cultures at a single-cell level (Fig. 2B). Objective quantification of oil red O staining, however, demonstrated statistically significant decreases in all NRTI-treated cultures (Fig. 2C). We then calculated the percentage of dead cells every 5 days and performed the final calculation of viable cells by exclusion of the cumulative percentage of dead cells for the entire period. After the culture of phsPA for 30 days in the presence of AZT, d4T, or ddC, we observed a moderate cumulative decrease in cell viability compared to that of the control (Fig. 2D). Similar cell death rates were observed when proliferating or fully differentiated phsPA were exposed to drugs (data not shown). When the findings are considered together and after adjustment for cumulative cell death, they show no decrease in the oil red O staining (Fig. 2C, dotted bars).

NRTI effects on adipogenic marker expression in differentiating phsPA. The findings described above suggested that the reduced oil red O staining was the effect of reduced cell numbers' leading to a decrease in total cytoplasmic triacylglyceride per culture flask rather than the effect of a decline in total cytoplasmic triacylglyceride per cell. To further analyze the effects of NRTI on adipogenic conversion, we measured the expression levels of the adipogenic transcription factors PPARγ and C/EBPα on day 18, a time point corresponding to

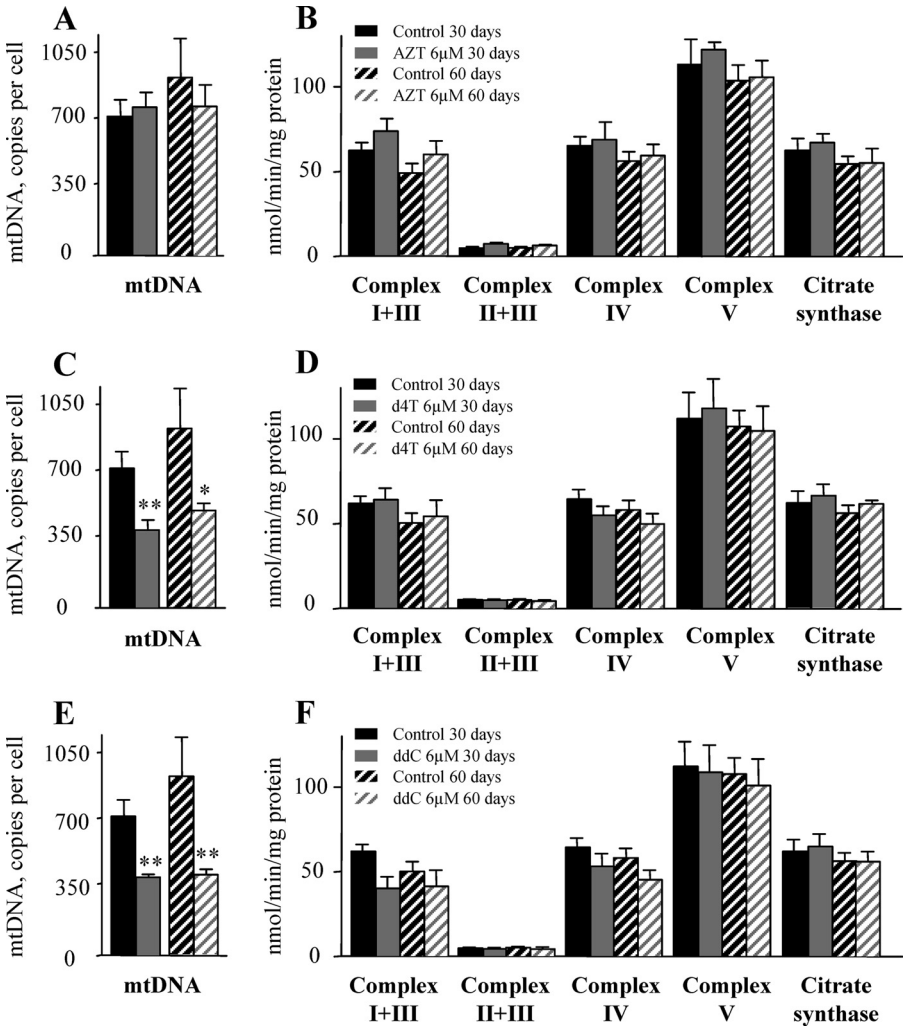

FIG. 3. Effects of NRTI on mtDNA content and on the respiratory chain complex activity in differentiating phsPA. (A, C, and E) The mtDNA contents of phsPA differentiated and further incubated till day 30 or 60 in the presence of 6 μM AZT (A), 3 μM d4T (C), or 0.1 μM ddC (E) or vehicle were measured using real-time PCR. (B, D, and F) Respiratory chain complex and citrate synthase activities under the culture conditions described above. Cells were sonicated, and individual substrates were added to the cell lysates, after which levels of substrate conversion by the respiratory chain complexes I and III, II and III, IV, and V and citrate synthase were measured photometrically. All graphs depict data from three independent experiments. Values are means ± SEM. Student's *t* test and ANOVA with Bonferroni's post hoc analysis were performed for comparison. *, $P < 0.05$, and **, $P < 0.01$ for comparison to control data.

complete adipocyte maturation (26, 31, 37). Day 18 of the differentiation protocol corresponds to a time point when a plateau of maturation is reached and is an appropriate point for the analysis of adipogenic transcription factors. At that time point, d4T- and ddC-treated cultures presented normal expression of PPARγ and C/EBPα (Fig. 2E and F). Incubation with AZT resulted in almost 40% decreases in the expression levels of these transcription factors, but these changes did not reach statistical significance under our experimental conditions (Fig. 2E and F). Interestingly, AZT has the capability of disturbing adipogenesis at least in murine cell lines, as we have described previously (28–30). Thus, we cannot exclude some minor effect of AZT on adipogenesis during longer incubation or in the presence of higher drug concentrations. Analyses of the expression and secretion of adiponectin at the end of 30 days of incubation with NRTI revealed no effect on the production of this insulin-sensitizing adipokine (Fig. 2G and H). Most of the dead cells detach and are lost during medium changes. We cannot exclude the possibility that the reduced number of viable cells (Fig. 2D) might have affected the measurement of adiponectin secretion into the cell culture supernatant to some extent (Fig. 2H). However, given that there was no significant decrease in adiponectin expression (Fig. 2G), which is not influenced by cell death, we conclude that there was no major impact on the level of adiponectin secretion per cell. Similarly, expression data presented in Fig. 2E, F, and G are not expected to be influenced by cell death rates, as they are likewise normalized on a per-cell basis by using a housekeeping gene.

Effects of NRTI on mtDNA content and respiratory chain function in differentiating phsPA. To study the effects of NRTI treatment on mitochondrial function, we first evaluated the

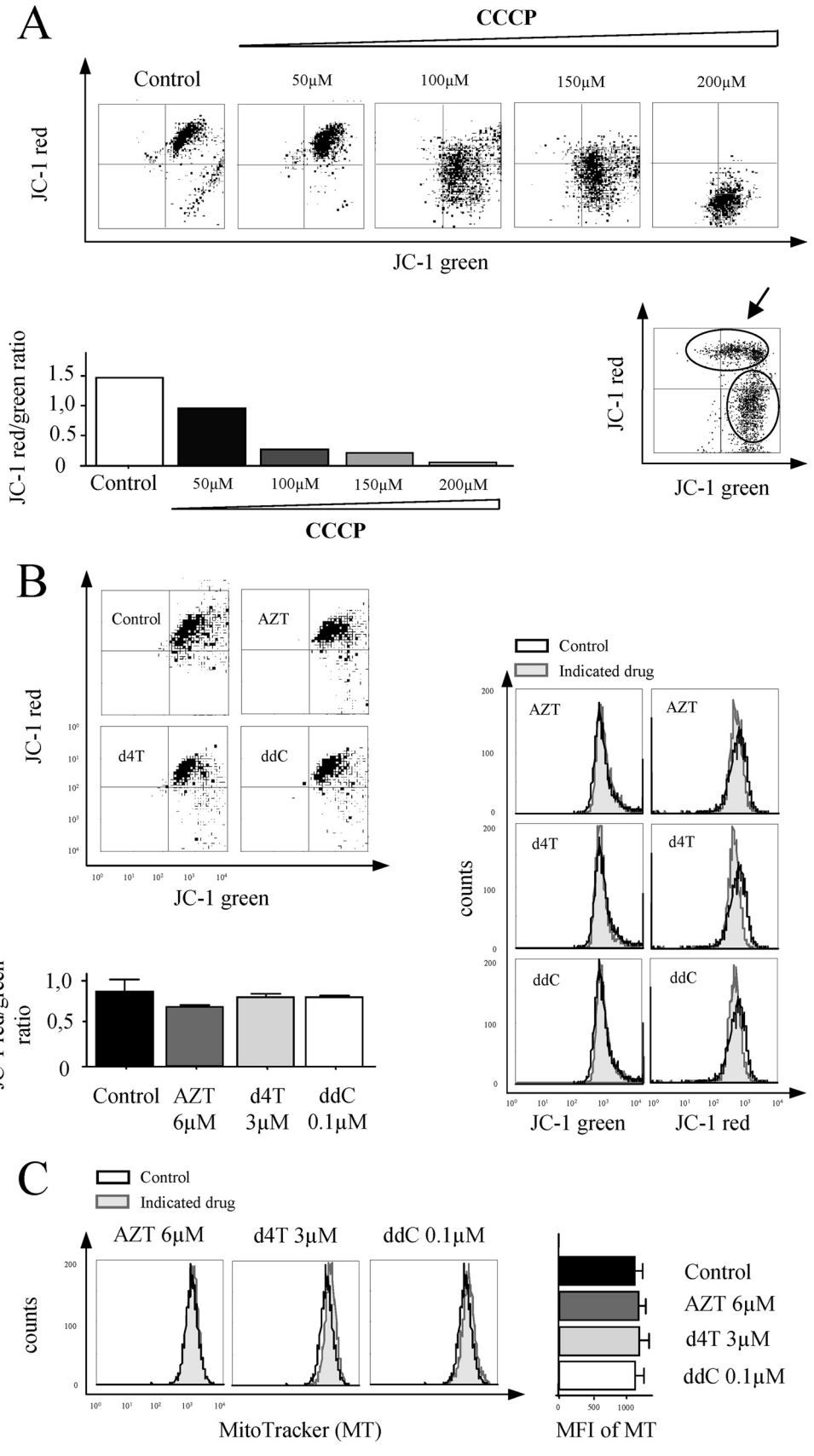
A
CCCP
Control
50μM
100μM
150μM
200μM
JC-1 red
JC-1 green
JC-1 red/green ratio
1.5
1,0
0.5
0
Control
50μM
100μM
150μM
200μM
CCCP
JC-1 red
JC-1 green
B
Control
AZT
d4T
ddC
JC-1 red
JC-1 green
Control
Indicated drug
AZT
AZT
d4T
d4T
ddC
ddC
counts
JC-1 red/green ratio
1,0
0,5
0
Control
AZT 6μM
d4T 3μM
ddC 0.1μM
JC-1 green
JC-1 red
C
Control
Indicated drug
AZT 6μM
d4T 3μM
ddC 0.1μM
counts
MitoTracker (MT)
Control
AZT 6μM
d4T 3μM
ddC 0.1μM
MFI of MT

effects of NRTI on phsPA differentiated and subsequently cultured in the presence of AZT, d4T, or ddC for a period of up to 30 days (Fig. 1). In additional experiments, the period of incubation with NRTI was extended to 60 days in order to examine long-term effects of the drugs. At therapeutic drug concentrations, AZT did not affect mtDNA abundance (Fig. 3A), which was significantly decreased in both d4T- and ddC-treated cultures (Fig. 3C and E) after 30 days of incubation. There was no further mtDNA depletion when treatment was extended to 60 days. Given the substantial mtDNA depletion after incubation with d4T and ddC, we performed experiments to assess whether this depletion translates into functional impairment of the respiratory chain complex activity. As depicted in Fig. 3C and E, under conditions leading to an approximately 50% reduction in the mtDNA copy number per cell (exposure to d4T and ddC), we did not detect measurable impairment of any respiratory chain complex activity (Fig. 3D and F). Similarly, citrate synthase activity as a mitochondrial marker was not affected in NRTI-treated cultures (Fig. 3B, D, and F). Corresponding results were obtained using proliferating preadipocytes in the presence of AZT (6 μM), d4T (3 μM), and ddC (0.1 μM) in samples for which we had previously confirmed mtDNA depletion by d4T and ddC (data not shown). We consider it unlikely that the reduced number of viable cells (Fig. 2D) has influenced the measurements for mtDNA abundance (Fig. 3A, C, and E) and respiratory chain complex activity (Fig. 3B, D, and F), as these values are normalized on a per-cell basis by using nuclear DNA and total cellular protein, respectively.

Impacts of NRTI on mitochondrial membrane potential and mitochondrial mass in phsPA. Given the NRTI-mediated mtDNA depletion without measurable impairment of any respiratory chain complex activity, we next assessed whether mitochondrial membrane potential or mitochondrial mass was affected. We decided to use flow cytometry for JC-1 red/green fluorescence measurement, which would allow us careful discrimination between a shift in fluorescence due to reduced potential in the total cell population (Fig. 4A, upper histograms) and reduced JC-1 red/green fluorescence due to cell death (Fig. 4A, lower right histogram). Our results from flow cytometry analyses confirmed the preservation of mitochondrial membrane potential (Fig. 4B) and normal mitochondrial mass (Fig. 4C) in cell cultures treated with AZT (6 μM), d4T (3 μM), and ddC (0.1 μM). These results demonstrated that 50% mtDNA depletion resulting from incubation with d4T and ddC at levels equivalent to the C_{max} is not associated with mitochondrial depolarization under the conditions used here.

DISCUSSION

Mitochondrial involvement in the pathogenesis of HIV-associated lipodystrophy has been suspected. Several studies have shown decreases in mtDNA levels in subcutaneous adipose tissues from lipoatrophic patients taking NRTI (12, 21). This depletion has been proposed to contribute to the pathogenesis of HIV lipodystrophy, although the extent and specificity of this effect remain unknown. If indeed mtDNA depletion was a crucial pathogenic factor, we expected to find the activities of complexes I, III, IV, and V of the respiratory chain to be significantly reduced since they are partially encoded by mitochondrial genes.

Impaired expression of adipogenic markers in subcutaneous abdominal adipose tissues from HIV-1-infected patients with peripheral lipoatrophy has been described previously (2), and impaired differentiation has been hypothesized to be one of the reasons for fat tissue atrophy (27). However, considering the multiple drugs, the HIV infection, and several metabolic factors characteristic of the in vivo situation, we performed in vitro analyses in order to examine the potential contribution of NRTI. Similar to the researchers in a recent in vitro study employing phsPA derived from healthy donors (26), we were unable to detect any disturbance in phsPA adipogenesis as a result of incubation with d4T. Unaffected adipogenesis has been proven at several independent levels. First, the acquisition of a mature phenotype and differentiation-dependent triacylglyceride accumulation were unaffected. Second, the expression of adipogenic transcription factors and the adipogenic marker adiponectin was normal. In addition, these results are in line with our earlier observations for 3T3-L1 and 3T3-F442A cell lines (28, 29). The effect of AZT on the differentiation-related expression of adipogenic transcription factors in phsPA was less pronounced than the effect in murine cell lines and suggested that phsPA might be less sensitive than the murine cells to AZT antiadipogenic effects. One potential explanation may be the lack of a clonal expansion stage in the in vitro differentiation of phsPA (22), since as we have demonstrated earlier, clonal expansion is one stage at which AZT affects adipogenesis (29). On the other hand, the differentiation of primary preadipocytes requires either indomethacin or rosiglitazone input. Some authors have speculated that the

FIG. 4. Effects of NRTI on mitochondrial membrane potential and mitochondrial mass in phsPA. (A) Upper histograms demonstrate a shift in the mitochondrial membrane potential in the total cell population induced by the mitochondrial membrane potential disrupter carbonyl cyanide 3-chlorophenylhydrazone (CCCP). Mitochondrial depolarization is indicated by a decrease in the JC-1 red/green fluorescence intensity ratio, presented in lower left graph. The lower right histogram shows data for a phsPA culture containing cells with normal potential (indicated by the arrow) and a high proportion of artificially induced cell death. (B) Upper left histograms are representative of the effects of 30 days of incubation with AZT (6 μM), d4T (3 μM), and ddC (0.1 μM) on mitochondrial membrane potential in phsPA. The potential shift in JC-1 red and green fluorescence intensity in the total cell population is depicted in the histograms on the right. The lower left graph summarizes the effects of 30 days of incubation with NRTI at levels equivalent to the C_{max} on mitochondrial membrane potential, indicated by the JC-1 red/green fluorescence intensity ratio. (C) Mitochondrial mass (indicated by MitoTracker staining) in phsPA after 30 days in the absence or presence of AZT, d4T, or ddC as detected by flow cytometry. Histograms on the left present results representative of MitoTracker fluorescence distribution at the cellular level. The graph on the right depicts the mean fluorescence intensity (MFI) for MitoTracker. The bar graphs in panels B and C represent results from three independent experiments. Values are means ± SEM. ANOVA with Bonferroni's post hoc analysis was performed for comparison. *, $P < 0.05$ for comparison to control data.

presence of substances with PPARγ-agonistic properties may explain the absence of an effect of the antiretroviral drugs (26). However, in the in vitro experiments demonstrating the consistent lack of an inhibitory effect of d4T on 3T3-L1 and 3T3-F442A cells, no such agonists were present (28, 29). In addition, the presence of rosiglitazone during the differentiation of 3T3-F442A cells in the presence of AZT was unable to rescue adipogenic conversion (30). The fact that in our experimental system adipocytes preserved normal expression and presumably normal secretion of adiponectin after exposure to NRTI supports the idea that the in vivo decrease in serum adiponectin levels may be more a result of comedication or of fat tissue atrophy than of NRTI-mediated decreased production on a cellular level. The moderate decrease in cell viability that we observed in vitro may be an additional factor.

In this study, using a sensitive functional assay, we obtained data providing evidence that significant mtDNA depletion may coexist with normal mitochondrial function and macroscopic integrity in phsPA and adipocytes, at least for the time period and under the conditions studied here. These results complement our previous findings obtained using the murine 3T3-L1 cell line (28). We wish to emphasize that in accordance with our hypothesis and our aim to study the mechanism of NRTI-induced mitochondrial dysfunction, we anticipated that it might be advantageous to avoid exceeding the therapeutically observed d4T C_{max} of about 2.5 μM, as discussed in reference 29, in order to be able to discern mechanisms of NRTI-induced mitochondrial dysfunction and depolarization without blurring the experimental outcomes with massive toxicity and cell death. Previous studies examined the effects of d4T at a concentration several times higher than the C_{max} (10 μM) on murine 3T3-F442A cells (5, 17, 32), as well as on human fibroblasts and adipocytes (6, 18). At this drug concentration, the authors detected a severalfold increase in death among 3T3-F442A cells (5) and about a 30% decrease in the survival rate of the human primary adipocytes during only 48 h of incubation (18). This high toxicity, combined with the fact that cell death and apoptosis are related to changes in mitochondrial depolarization (Fig. 4A), can make the causal interpretation of changes in JC-1 red/green fluorescence difficult. We aimed to reduce this bias by using flow cytometry and by limiting the NRTI toxicity with a drug concentration close to the C_{max}.

The proof that mtDNA depletion is a relevant cause for mitochondrial and adipocyte dysfunction is fundamental for the understanding of the pathogenesis of lipoatrophy (4) and is also important for therapeutic consequences. Various nonadipocyte studies suggested mitochondrial threshold effects (24); however, there is limited information regarding the relevance of such thresholds for adipocytes. Other nonadipocyte studies demonstrated that when mitochondrial replication and protein synthesis are severely inhibited by ethidium bromide and chloramphenicol, there is progressive dose-dependent decrease in cytochrome oxidase and succinate-cytochrome *c* reductase activities (16). Given that such relationships are difficult to extrapolate, as they seem to be agent and cell type specific, our aim was to investigate the relationship between NRTI-mediated mtDNA depletion and mitochondrial function in primary human subcutaneous adipocytes. Our experiments demonstrated that even after prolonged NRTI exposure and despite a 50% mtDNA reduction, mitochondrial function appears to be maintained in adipocytes. Given that severe lipoatrophy in association with 43% mtDNA depletion in NRTI-treated HIV-positive patients has been reported previously (34), we consider the 50% depletion in our model closely resembling in vivo observations. It is reasonable to speculate that in vivo, additional factors like the HIV infection itself (8, 9) or hepatitis C virus infection (33) may potentially exacerbate any effect on mitochondria and further decrease the mtDNA content.

The present study overcomes some limitations of the systems used in previous analyses (28). The use of a human primary cell culture facilitates direct extrapolation to the human in vivo situation. It also better accounts for significant differences in cellular drug uptake and phosphorylation. However, several differences in terms of the time course of the drug concentration (levels of NRTI in plasma show a short half-life), the time of drug exposure, and the lack of secondary factors such as cytokines and viral infection still have to be considered. Alternatively, the half-lives of respiratory chain complexes may be longer and reduced activities of respiratory chain complexes may develop later in cell life. The data we provide here exclude possible species-specific differences in enzymatic activity for drug phosphorylation or the dependency of adipocyte function on mtDNA content, which have not been addressed using the 3T3-L1 murine cell line model. The use of primary cultures also excludes differences that may arise from immortalized murine cell lines.

In summary, our results suggest that NRTI at therapeutic doses reduce mtDNA abundance in a primary human adipocyte culture model and that this depletion appears to be a poor predictor for mitochondrial dysfunction. These data have important implications for the understanding and treatment of the HIV therapy-associated lipodystrophy syndrome.

ACKNOWLEDGMENT

This work was supported by H. W. & J. Hector Stiftung.

REFERENCES

1. **Addy, C. L., A. Gavrila, S. Tsiodras, K. Brodovicz, A. W. Karchmer, and C. S. Mantzoros.** 2003. Hypoadiponectinemia is associated with insulin resistance, hypertriglyceridemia, and fat redistribution in human immunodeficiency virus-infected patients treated with highly active antiretroviral therapy. J. Clin. Endocrinol. Metab. **88:**627–636.
2. **Bastard, J. P., M. Caron, H. Vidal, V. Jan, M. Auclair, C. Vigouroux, J. Luboinski, M. Laville, M. Maachi, P. M. Girard, W. Rozenbaum, P. Levan, and J. Capeau.** 2002. Association between altered expression of adipogenic factor SREBP1 in lipoatrophic adipose tissue from HIV-1-infected patients and abnormal adipocyte differentiation and insulin resistance. Lancet **359:** 1026–1031.
3. **Bensadoun, A., and D. Weinstein.** 1976. Assay of proteins in the presence of interfering materials. Anal. Biochem. **70:**241–250.
4. **Brinkman, K., J. A. Smeitink, J. A. Romijn, and P. Reiss.** 1999. Mitochondrial toxicity induced by nucleoside-analogue reverse-transcriptase inhibitors is a key factor in the pathogenesis of antiretroviral-therapy-related lipodystrophy. Lancet **354:**1112–1115.
5. **Caron, M., M. Auclair, C. Lagathu, A. Lombes, U. A. Walker, M. Kornprobst, and J. Capeau.** 2004. The HIV-1 nucleoside reverse transcriptase inhibitors stavudine and zidovudine alter adipocyte functions in vitro. AIDS **18:**2127–2136.
6. **Caron, M., M. Auclairt, A. Vissian, C. Vigouroux, and J. Capeau.** 2008. Contribution of mitochondrial dysfunction and oxidative stress to cellular premature senescence induced by antiretroviral thymidine analogues. Antivir. Ther. **13:**27–38.
7. **Carr, A.** 2003. HIV lipodystrophy: risk factors, pathogenesis, diagnosis and management. AIDS **17**(Suppl. 1)**:**S141–S148.
8. **Casula, M., I. Bosboom-Dobbelaer, K. Smolders, S. Otto, M. Bakker, M. P. de Baar, P. Reiss, and A. de Ronde.** 2005. Infection with HIV-1 induces a decrease in mtDNA. J. Infect. Dis. **191:**1468–1471.
9. **Cote, H. C., Z. L. Brumme, K. J. Craib, C. S. Alexander, B. Wynhoven, L.**

Ting, H. Wong, M. Harris, P. R. Harrigan, M. V. O'Shaughnessy, and J. S. Montaner. 2002. Changes in mitochondrial DNA as a marker of nucleoside toxicity in HIV-infected patients. N. Engl. J. Med. **346:**811–820.
10. **Das, A. M., D. J. Byrd, and J. Brodehl.** 1994. Regulation of the mitochondrial ATP-synthase in human fibroblasts. Clin. Chim. Acta **231:**61–68.
11. **Faloona, G. R., and P. A. Srere.** 1969. Escherichia coli citrate synthase. Purification and the effect of potassium on some properties. Biochemistry **8:**4497–4503.
12. **Hammond, E., D. Nolan, I. James, C. Metcalf, and S. Mallal.** 2004. Reduction of mitochondrial DNA content and respiratory chain activity occurs in adipocytes within 6–12 months of commencing nucleoside reverse transcriptase inhibitor therapy. AIDS **18:**815–817.
13. **John, M., E. J. McKinnon, I. R. James, D. A. Nolan, S. E. Herrmann, C. B. Moore, A. J. White, and S. A. Mallal.** 2003. Randomized, controlled, 48-week study of switching stavudine and/or protease inhibitors to combivir/abacavir to prevent or reverse lipoatrophy in HIV-infected patients. J. Acquir. Immune Defic. Syndr. **33:**29–33.
14. **Joly, V., P. Flandre, V. Meiffredy, N. Leturque, M. Harel, J. P. Aboulker, and P. Yeni.** 2002. Increased risk of lipoatrophy under stavudine in HIV-1-infected patients: results of a substudy from a comparative trial. AIDS **16:**2447–2454.
15. **Kim, M. J., C. Jardel, C. Barthélémy, V. Jan, J.-P. Bastard, S. Chapin, S. Houry, P. Levan, J. Capeau, and A. Lombès.** 2005. Preserved cytochrome c oxidase activity despite mitochondrial DNA depletion in adipose tissue of HIV-infected patients with lipodystrophy. Antivir. Ther. **10**(Suppl. 3)**:**L8.
16. **King, M. E., G. C. Godman, and D. W. King.** 1972. Respiratory enzymes and mitochondrial morphology of HeLa and L cells treated with chloramphenicol and ethidium bromide. J. Cell Biol. **53:**127–142.
17. **Lagathu, C., J. P. Bastard, M. Auclair, M. Maachi, M. Kornprobst, J. Capeau, and M. Caron.** 2004. Antiretroviral drugs with adverse effects on adipocyte lipid metabolism and survival alter the expression and secretion of proinflammatory cytokines and adiponectin in vitro. Antivir. Ther. **9:**911–920.
18. **Lagathu, C., B. Eustace, M. Prot, D. Frantz, Y. Gu, J. P. Bastard, M. Maachi, S. Azoulay, M. Briggs, M. Caron, and J. Capeau.** 2007. Some HIV antiretrovirals increase oxidative stress and alter chemokine, cytokine or adiponectin production in human adipocytes and macrophages. Antivir. Ther. **12:**489–500.
19. **Lewis, W.** 2005. Nucleoside reverse transcriptase inhibitors, mitochondrial DNA and AIDS therapy. Antivir. Ther. **10:**M13–M27.
20. **Lucke, T., W. Hoppner, E. Schmidt, S. Illsinger, and A. M. Das.** 2004. Fabry disease: reduced activities of respiratory chain enzymes with decreased levels of energy-rich phosphates in fibroblasts. Mol. Genet. Metab. **82:**93–97.
21. **McComsey, G. A., D. M. Paulsen, J. T. Lonergan, S. M. Hessenthaler, C. L. Hoppel, V. C. Williams, R. L. Fisher, C. L. Cherry, C. White-Owen, K. A. Thompson, S. T. Ross, J. E. Hernandez, and L. L. Ross.** 2005. Improvements in lipoatrophy, mitochondrial DNA levels and fat apoptosis after replacing stavudine with abacavir or zidovudine. AIDS **19:**15–23.
22. **Newell, F. S., H. Su, H. Tornqvist, J. P. Whitehead, J. B. Prins, and L. J. Hutley.** 2006. Characterization of the transcriptional and functional effects of fibroblast growth factor-1 on human preadipocyte differentiation. FASEB J. **20:**2615–2617.
23. **Nolan, D., E. Hammond, A. Martin, L. Taylor, S. Herrmann, E. McKinnon, C. Metcalf, B. Latham, and S. Mallal.** 2003. Mitochondrial DNA depletion and morphologic changes in adipocytes associated with nucleoside reverse transcriptase inhibitor therapy. AIDS **17:**1329–1338.
24. **Rossignol, R., B. Faustin, C. Rocher, M. Malgat, J. P. Mazat, and T. Letellier.** 2003. Mitochondrial threshold effects. Biochem. J. **370:**751–762.
25. **Rozen, S., and H. Skaletsky.** 2000. Primer3 on the WWW for general users and for biologist programmers. Methods Mol. Biol. **132:**365–386.
26. **Saillan-Barreau, C., O. Tabbakh, J. P. Chavoin, L. Casteilla, and L. Penicaud.** 2008. Drug-specific effect of nelfinavir and stavudine on primary culture of human preadipocytes. J. Acquir. Immune Defic. Syndr. **48:**20–25.
27. **Stankov, M. V., and G. M. Behrens.** 2007. HIV-therapy associated lipodystrophy: experimental and clinical evidence for the pathogenesis and treatment. Endocr. Metab. Immune Disord. Drug Targets **7:**237–249.
28. **Stankov, M. V., T. Lucke, A. M. Das, R. E. Schmidt, and G. M. Behrens.** 2007. Relationship of mitochondrial DNA depletion and respiratory chain activity in preadipocytes treated with nucleoside reverse transcriptase inhibitors. Antivir. Ther. **12:**205–216.
29. **Stankov, M. V., R. E. Schmidt, and G. M. Behrens.** 2008. Zidovudine impairs adipogenic differentiation through inhibition of clonal expansion. Antimicrob. Agents Chemother. **52:**2882–2889.
30. **Stankov, M. V., R. E. Schmidt, and G. M. Behrens.** 2009. Combined effect of C-reactive protein and stavudine on adipogenesis. Antivir. Ther. **14:**819–829.
31. **Vernochet, C., S. Azoulay, D. Duval, R. Guedj, F. Cottrez, H. Vidal, G. Ailhaud, and C. Dani.** 2005. Human immunodeficiency virus protease inhibitors accumulate into cultured human adipocytes and alter expression of adipocytokines. J. Biol. Chem. **280:**2238–2243.
32. **Walker, U. A., M. Auclair, D. Lebrecht, M. Kornprobst, J. Capeau, and M. Caron.** 2006. Uridine abrogates the adverse effects of antiretroviral pyrimidine analogues on adipose cell functions. Antivir. Ther. **11:**25–34.
33. **Walker, U. A., J. Bauerle, M. Laguno, J. Murillas, S. Mauss, G. Schmutz, B. Setzer, R. Miquel, J. M. Gatell, and J. Mallolas.** 2004. Depletion of mitochondrial DNA in liver under antiretroviral therapy with didanosine, stavudine, or zalcitabine. Hepatology **39:**311–317.
34. **Walker, U. A., M. Bickel, S. I. Lutke Volksbeck, U. P. Ketelsen, H. Schofer, B. Setzer, N. Venhoff, V. Rickerts, and S. Staszewski.** 2002. Evidence of nucleoside analogue reverse transcriptase inhibitor-associated genetic and structural defects of mitochondria in adipose tissue of HIV-infected patients. J. Acquir. Immune Defic. Syndr. **29:**117–121.
35. **Walker, U. A., B. Setzer, and N. Venhoff.** 2002. Increased long-term mitochondrial toxicity in combinations of nucleoside analogue reverse-transcriptase inhibitors. AIDS **16:**2165–2173.
36. **Yamauchi, T., J. Kamon, H. Waki, Y. Terauchi, N. Kubota, K. Hara, Y. Mori, T. Ide, K. Murakami, N. Tsuboyama-Kasaoka, O. Ezaki, Y. Akanuma, O. Gavrilova, C. Vinson, M. L. Reitman, H. Kagechika, K. Shudo, M. Yoda, Y. Nakano, K. Tobe, R. Nagai, S. Kimura, M. Tomita, P. Froguel, and T. Kadowaki.** 2001. The fat-derived hormone adiponectin reverses insulin resistance associated with both lipoatrophy and obesity. Nat. Med. **7:**941–946.
37. **Zen-Bio.** 30 June 2009, accession date. Subcutaneous human adipocytes: maintenance and differentiation from preadipocytes to adipocytes. Instruction manual ZBM0001.01. Zen-Bio, Inc., Research Triangle Park, NC. http://www.zen-bio.com/pdf/ZBM0001.01SQAdipocyteCareRV08.08.pdf.